Nanoscale

Accepted Manuscript

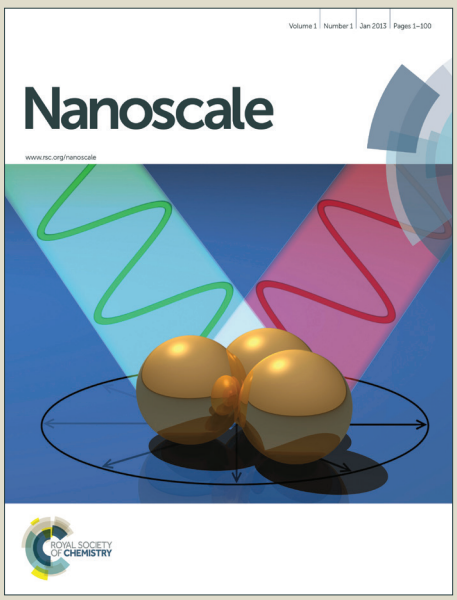

ROYAL SOCIETY OF CHEMISTRY

www.rsc.org/nanoscale

Self-Constructed Tree-Shape High Thermal Conductivity Nanosilver Networks in Epoxy

Kamyar Pashayi,[ǂ] Hafez Raeisi Fard,[†] Fengyuan Lai,[‡] Sushumna Iruvanti,[§] Joel Plawsky,[ǁ] Theodorian Borca-Tasciuc[†,]*

[ǂ] School of Science, Engineering, and Technology, Pennsylvania State University, Middletown, PA 17057-4846, USA

[†] Department of Mechanical, Aerospace, and Nuclear Engineering, Rensselaer Polytechnic Institute, Troy, NY 12180-3590, USA

[‡] Department of Materials Science and Engineering, Rensselaer Polytechnic Institute, Troy, NY 12180-3590, USA

[§] IBM Systems & Technology Group, Hopewell Junction, NY 12533, USA

[ǁ] Department of Chemical and Biological Engineering, Rensselaer Polytechnic Institute, Troy, NY 12180-3590, USA

KEYWORDS: Self-assembly, nanocomposite, thermal conductivity, sintering

Graphical Abstract

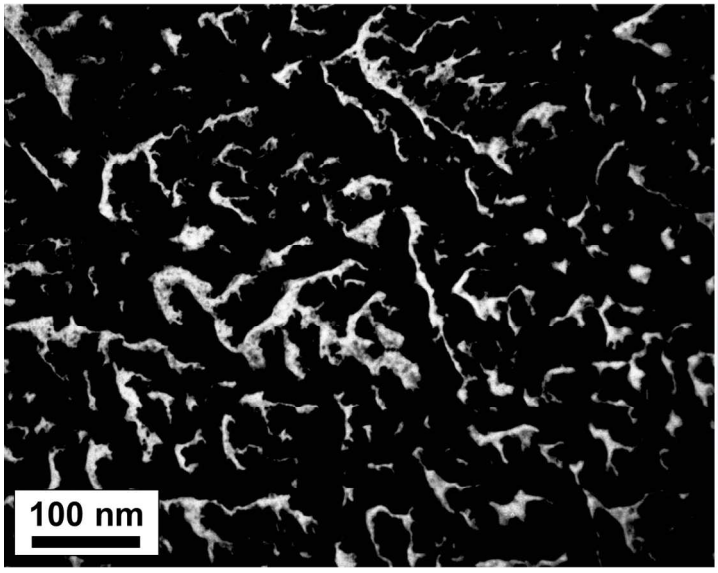

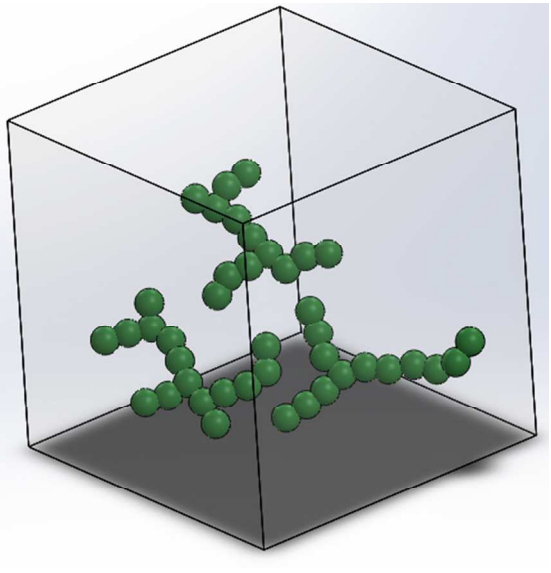

Abstract

We report the formation of high aspect ratio nanoscale tree-shape silver networks in epoxy, at low temperatures (<150 ºC) and atmospheric pressure, that are correlated to a ~200 folds enhancement of thermal conductivity (κ) of the nanocomposite vs. the polymer matrix. The networks form through a three-step process comprising of self-assembly by diffusion limited aggregation of polyvinylpyrrolidone (PVP) coated nanoparticles, removal of PVP coating from the surface, and sintering of silver nanoparticles in high aspect ratio networked structures. Controlling self-assembly and sintering by carefully designed multistep temperature and time processing leads to κ for our silver nanocomposites that are up to 300% of the present state of the art for polymer nanocomposites at similar volume fractions. Our investigation of the κ enhancements enabled by tree-shape network nanocomposites provides a basis for development of new polymer nanocomposites for thermal transport and storage applications.

1. Introduction

Polymer composites containing metallic particles are commonly used in electronic, optoelectronic, photonic device packaging and other thermal management systems.[1,2,3] Low aspect ratio nanoparticles, coupled with poor thermal and electrical contact between particles and/or high interface thermal resistance between particles and matrix typically produce composites with low κ.[4,5] For a polymer-silver nanocomposite at 20 vol% nanoparticles, κ=6.5 $Wm^{-1}K^{-1}$ was reported,[6] which is much lower than the theoretical limit of κ~61 $Wm^{-1}K^{-1}$. On the other hand high aspect ratio metallic fillers such as nanowires can increase the composite thermal conductivity,[7] however they also greatly increase the viscosity of the uncured composites.[8,9] Our objective is to obtain a high κ nanocomposite without starting with nanowire fillers. We propose

that using self-assembly and sintering to bond neighboring particles into higher aspect ratio structures could alleviate the high viscosity of nanowire composites while still enhancing κ. Nanoparticle fillers are desirable since they can be sintered together at lower temperatures than microparticles.[10] Employing silver nanoparticle sintering and controlling the structure of nanocomposites to improve their properties has been mainly carried out for electrically conductive materials.[11,12,13] Our initial work has demonstrated that processing a silver nanoparticle composite in a one step 150 ºC process can lead to κ=17.6 $Wm^{-1}K^{-1}$ due to the formation of self-constructed high aspect ratio structures inside the matrix.[14] However, the mechanisms responsible for the structure formation and ways to maximize the effect were not investigated.

In this paper, we unearth the network formation mechanisms through a set of carefully designed processing-structure investigations and find key information for optimum processing of the nanocomposite to provide high thermal conductivity. We demonstrate the ability to change the size, shape, volume fraction, and degree of filler network formation. Microstructural visualization and κ measurements show that the maximum κ values are correlated to a tree-shape structure yielding κ enhancement of nanocomposites by a factor of ~200 compared to that of the matrix. Such key enhancements in nanocomposite properties open new pathways for commercial developments.[4]

2. Experimental

Samples were synthesized by mixing 20 vol% of silver nanoparticles with epoxy resin and curing agent (resin to hardener ratio of 10 to 8 by weight) using an ultrathin probe sonicator for 60 minutes. The silver nanoparticles were 20 nm in diameter and coated with 5 Å of PVP.

Transmission and Scanning Electron Micrographs of dry particles and after forming a slurry with uncured epoxy are shown in Figures 1a & 1b, respectively. In order to reveal the silver nanoparticles structure in image (b), the surface of the sample was etched using a methylene chloride epoxy remover solution. The porous background in image (b) is either due to trapped air bubbles during sonication or deep etching during SEM sample preparation. These images indicate that even though nanoparticles were clustered when in a dry form, ultrasonic mixing in the epoxy media results in particles dispersion.[1] PVP plays a crucial role in preventing surface oxidation and enabling particle dispersion in epoxy.[2] Mixing uncoated silver nanoparticles in epoxy results in poor dispersions as shown in the supporting information (see figure S1 and S2). The homogeneous slurry was loaded into a silicone mold, degassed in vacuum, and heated in a furnace for curing.[Error! Bookmark not defined.] In order to investigate the κ-structure interrelation, single step and multistep temperature processing conditions were investigated in synergy with microscopy, thermal conductivity and rheology experiments.

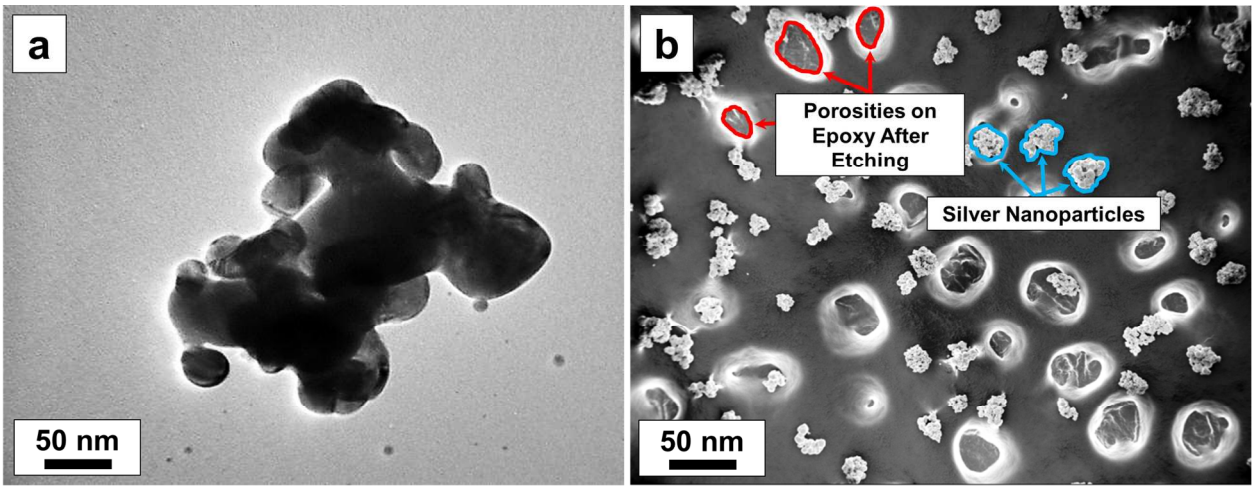

Figure 1. *(a) TEM image of a cluster of 20 nm diameter silver particles and (b) SEM image of dispersed 20 nm, 20 vol% silver-epoxy nanocomposite slurry (uncured) after sonication.*

3. Results and Discussion

The thermal conductivity of the nanocomposites was measured using a one-dimensional steady-state method developed by the authors based on an updated version of ASTM D5470.[14]

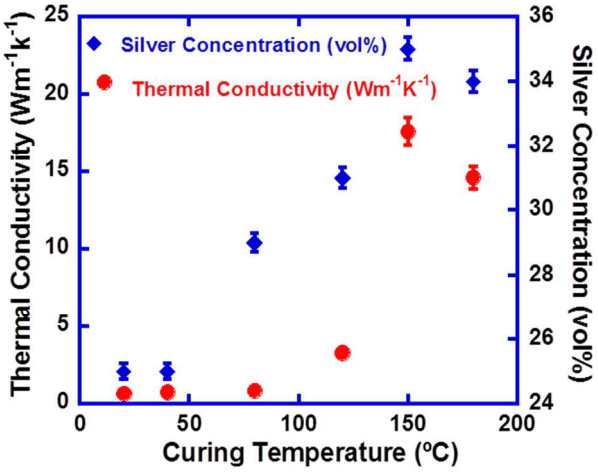

Figure 2. *Thermal conductivity and final silver concentration in the tested samples as a function of the curing temperature for one-step processing conditions.*

Initial clues of the structure formation mechanisms were gathered from investigations where the curing temperature was tested in the range between 20 ºC and 180 ºC. Curing times were varied between one hour to seven days depending on the curing temperature (see table S1 in the supporting information). The thermal conductivity values of the resulting nanocomposites are shown in Figure 2. The graph starts with a gradual increase in thermal conductivity with curing temperature followed by a sharp increase between 120 ºC to 150 ºC, then a slight decrease.

The thermal conductivity trends were correlated with SEM morphology analysis for the single-step temperature processing samples showed in Fig. 3. At curing temperatures below 150 ºC, the nanoparticles form isolated clusters, distributed homogeneously in the epoxy matrix.

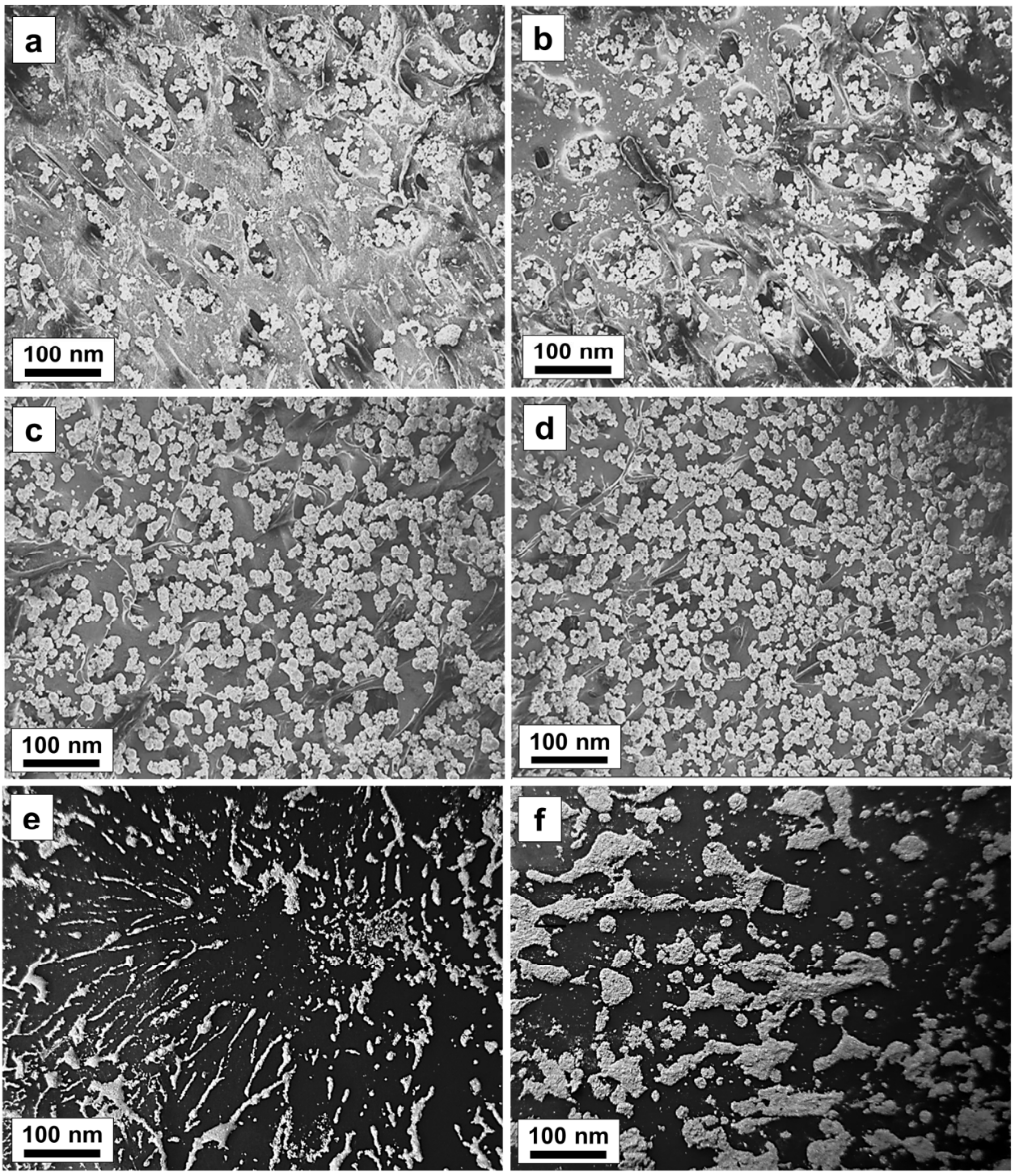

Figure 3. *SEM images of 20 nm silver-epoxy nanocomposites cured at (a) 20 ºC, (b) 40 ºC, (c) 80 ºC, (d) 120 ºC, (e) 150 ºC, and (f) 170 ºC.*

With increasing curing temperatures, the distance between the clusters decreases (see Figure 3a-d). The particle behavior in these samples (Figure 3a-d) can be explained as follows: The particles show a tendency for clustering.[15,16] As the clusters coalesce to form a connected network, the particles still remain separated and not sintered together because of low processing temperature. The starting silver concentration in these samples was 20 vol%. However, the SEM images shown in figure 3a-3d were taken from the bottom of the specimens where the silver nanoparticles have settled down and the volume fractions of silver are significantly higher.

Microstructural observations from Fig. 3e suggest that curing at 150 ºC for 60 minutes is adequate to form solid bridges between neighboring silver particles.[17] Moreover, at temperatures between 120 ºC and 150 ºC, the structure changes from not sintered particles to high aspect ratio structures accompanied by a rapid improvement in κ as observed in Figure 2. As implied by the successful sintering observed in Figure 3e and 3f, PVP removal from the particles, sintering of silver nanoparticles, and curing of epoxy should occur at both 150 ^{o}C and 180 ^{o}C. Most of the primary particles have formed a sintered self-assembled metallic structure. At 180 ^{o}C curing, the higher temperature amplifies the sintering rate and leads to growth in the radial direction versus axial direction and consequently the development of lower-aspect ratio structures. It is also possible that the faster curing rate for the epoxy at 180 ºC prevented the assembly of higher aspect ratio structures by locking in the structure too early. Since the samples cured at 150 ºC and 180 ºC have almost similar silver loadings of 35 vol% (ρ=4.45 g.cm^{-3}) and 34 vol% (ρ=4.33 g.cm^{-3}), respectively, the lower aspect ratio of the structures obtained at 180 ºC explains the decrease in κ. While curing temperature experiments point to 150 ^{o}C to be optimum for particle bridging, further experiments were conducted to understand the role of assembly and sintering and to provide a better control of the high thermal conductivity pathways.

To investigate the impact of time and temperature on the nanoparticle agglomeration process, an optical microscopy investigation was performed on a 20 vol% silver-epoxy slurry poured into a cubic glass container (6 cm×6 cm×0.5 cm) and exposed to heating on a hotplate. An E-type thermocouple was embedded in the slurry to read the temperature of the system. At room temperature, it was observed that over time the outer edges of the sample became depleted of silver particles as they migrated toward the center of the container (see the series of optical pictures in Figure S3 in the supporting information). After 60 minutes, the darker area does not shrink anymore inferring that the particles have reached an equilibrium distance from each other. The blue and black curves in Figure 4a represent respectively the normalized diameter of the dark region and the apparent volume fraction calculated from the micrograph of the agglomerated region. As the particles agglomerate with time, the normalized diameter of the dark region decreases and the corresponding apparent silver concentration increases locally from 20 vol% (ρ=3.05 g.cm^{-3}) to 23 vol% (ρ=3.33 g.cm^{-3}) as seen in Fig. 4a.

Next a ramp test with a rate of 1 ºC/min was performed on the same uncured slurry to study the rate of agglomeration as a function of temperature. The absolute value of the derivative of the diameter of the agglomerated region with respect to temperature (|dD/dT|) was extracted and plotted versus temperature in Figure 4b. The maximum rate of diameter change, indicating the maximum agglomeration rate was obtained at 100 ºC. The results in Fig. 4 imply that agglomeration of particles occurs in 60 minutes at room temperature and it is enhanced with temperature reaching a peak around at 100 ºC.

Since the assembly of nanoparticles into higher aspect ratio interconnected structures would increase the viscosity of uncured slurries, viscosity measurements were used to determine the time for agglomeration. As presented in Figure S4 in the supporting information, the viscosity of

pure epoxy remains constant (red line in Figure S4) at 100 ºC for extended periods of time. However, at the same temperature, the viscosity of the nanocomposite slurry increases from 0.15

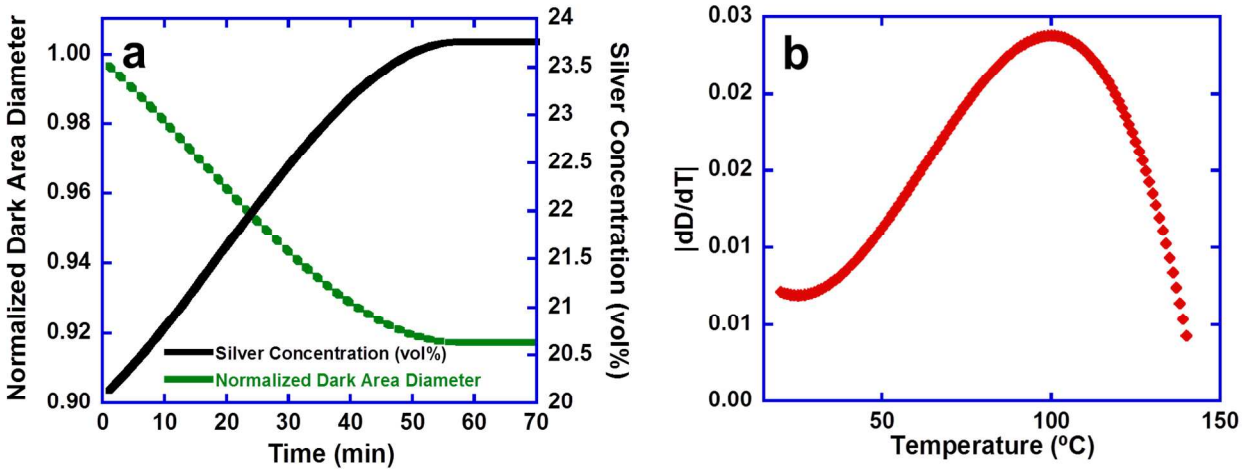

Figure 4. *Optical microscopy of silver nanoparticles in uncured epoxy showing: (a) the normalized diameter of the high silver nanoparticle concentration region (dark area) in the center of the sample versus time, taken at room temperature; (b) the rate of change with temperature of the dark area diameter |dD/dT| plotted versus temperature, taken during 1 ºC/min ramp-up tests. The fastest agglomeration rate occurs at ~ 100 ºC.*

Pa.s to 7.82 Pa.s in 60 minutes (green line Figure S4). These results indicate that the changes in viscosity are due to nanoparticle assembly and not due to epoxy curing. A similar order of magnitude for the agglomeration time was obtained theoretically by balancing Van der Waals forces against drag forces. This calculation is shown in section V in the supporting information.

The first part of the study indicates that achieving a high κ in a silver nanoparticles-epoxy composite requires: (*i*) Assembly of the particles through agglomeration before the epoxy was substantially cured and this process was identified to be optimal at 100 ºC for 20 nm silver-epoxy system. (*ii)* ungrafting the PVP coating from the surface of nanoparticles to promote lattice diffusion and surface fusion during nanoparticle sintering. Differential scanning calorimetry

(DSC) analysis of pure bulk PVP indicates a melting peak at 145 ºC with an onset temperature around 75 ºC (see Figure S5 in the supporting information). The more efficient the PVP removal,

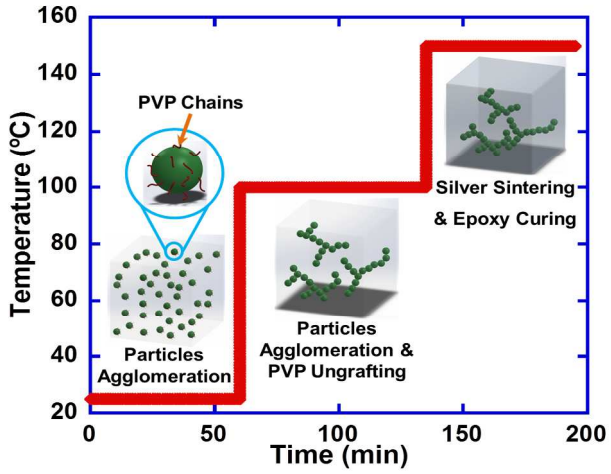

Figure 5. *Three-step optimum processing: (i) particle agglomeration at 20 ºC, (ii) PVP ungrafting at 100 ºC and (iii) particle sintering at 150 ºC.*

the faster would be the sintering.[18] (*iii*) processing at 150 ºC for sintering of silver particles, and epoxy curing, for optimal heat transfer pathways in the 20 nm silver-epoxy system. Based on these requirements a three-step composite fabrication and particle network formation was developed as shown in Figure 5.

In order to refine the time at 100 ºC for particle agglomeration and PVP ungrafting, experiments were carried out with varying time for the agglomeration step. SEM images of cured nanocomposites prepared following the three-step methodology versus the agglomeration/PVP removal time at 100 ºC are shown in Figure 6. These images show that as time for the agglomeration/PVP removal step increases, longer and narrower self-assembled fractal tree shape structures emerge.

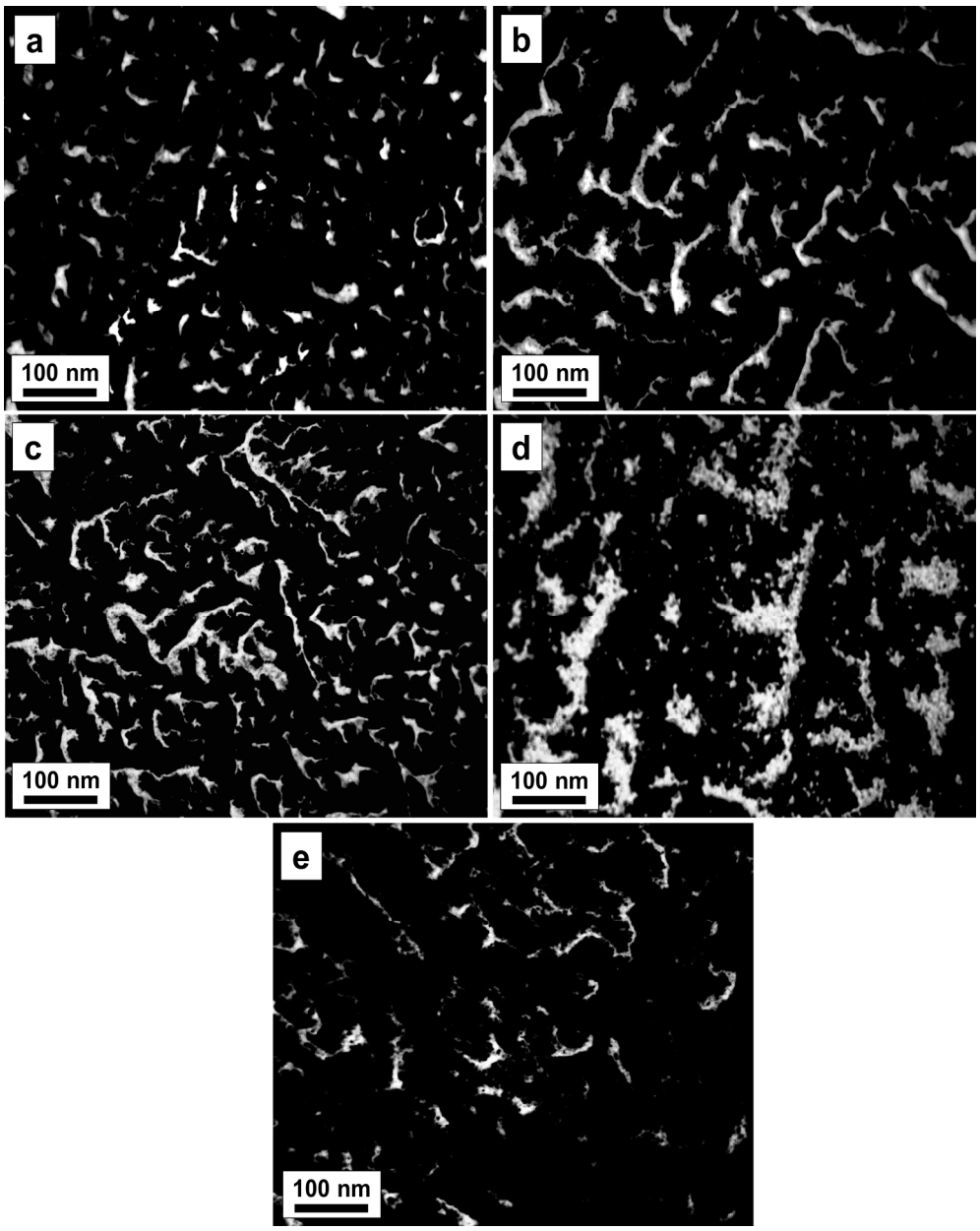

Figure 6. *SEM images of silver-epoxy nanocomposites prepared using the three step process from Fig. 5 and a variable dwell time at 100 ºC of: (a) 15min, (b) 30min, (c) 60min and (d) 90 min. The initial silver concentration was 20 vol% for figures 6a-6d. Thermal conductivity measurements indicate 60min as optimum for at this concentration. Figure 6e is the SEM image of a sample prepared based on optimum three-step processing with initial silver loading of 6 vol% and final silver concentration of 10 vol%.*

These shapes resemble structures in diffusion-limited aggregation (DLA) processes, as theoretically studied by Witten and Sander in 1981.[19] DLA has been applied for developing dendritic fractal structures of silver particles in electroreduction[20] and electrodeposition[21] applications, and in the synthesis of chainlike nanostructures.[22] However, increasing the processing time beyond 60 minutes (90 minutes) for the agglomeration step leads to a lower aspect ratio structure as observed in Figure 6d. The longer time allows the particles to form a thicker network at the expense of a shorter lengths resulting in a lower aspect ratio global network structure. From Fig. 6a-d, we observed that the highest aspect ratio fractal is reached for 60 minutes agglomeration step highlighting an optimum time for interconnected network structure formation. In accordance with the expectation of a high composite κ with high aspect ratio fractals, samples processed at 60 minutes 100 ºC for agglomeration step and 60 minutes 150 ºC for sintering step also resulted in the highest κ=38.50 $Wm^{-1}K^{-1}$ for our nanocomposite (~10% of metallic silver's bulk κ). The high composite κ is attributed to: (*i*) heat flow along high aspect ratio high thermal conductivity structures (the backbone of the fractals) and (*ii*) a reduction in the interfacial thermal resistance due to enhanced particle-particle contact in the network.[23] The final silver concentration of the sample shown in figure 6c is 48 vol% (ρ=5.65 $g.cm^{-3}$) derived from the bottom half of the 20 vol% sample.

The structure of the nanocomposite shown in figure 6e is for a 10 vol% silver concentration (starting concentration 6%). Thermal measurements yielded κ=12.05 $Wm^{-1}K^{-1}$ for this composite which is >3 times the value[14] (12.05 $Wm^{-1}K^{-1}$ vs. 3.19 $Wm^{-1}K^{-1}$) obtained from one-step processing at 150 ºC. The results indicate that using the optimized processing method proposed in Figure 5 had a strong beneficial impact on κ enhancement of nanocomposites.

In the comparison chart shown in Fig. 7 the thermal conductivity of the 10% silver-epoxy composite is ~3 times the reported value for the state of the art composite at the same volume fraction, a 10 vol.% graphene-epoxy (G-EP) composite.[24] At 48 vol.% silver loading, we measured a 54% larger value relative to the state of the art (38.50 $Wm^{-1}K^{-1}$ vs. 25 $Wm^{-1}K^{-1}$), for

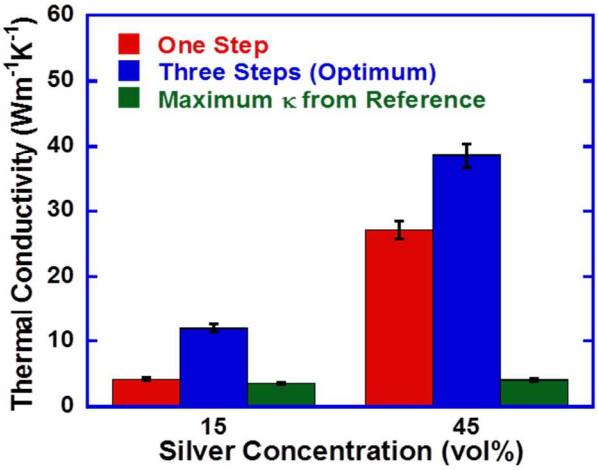

Figure 7. *Comparison of the thermal conductivity of epoxy/silver nanocomposites made with one-step (150 ºC curing) and three-step processing. Literature values for thermal conductivity of state of the art polymer composites at the same or larger volume fractions of fillers are included for comparison from references 24 and 25.*

a vapor grown carbon fiber-epoxy (VGCF-EP) composite at similar filler loading (45 vol%).[25] Moreover, our maximum κ value is 18 % larger than the maximum κ value reported so far for a polymer composite, 32.5 $Wm^{-1}K^{-1}$ for a large volume fraction (78.5) BN-polybenzoxazine composite, where the particle size of BN was also a significantly much larger, 225 μm.[26]

4. Conclusions

In summary, a set of carefully designed experiments were conducted to understand the mechanism of large κ enhancements in a silver-epoxy nanocomposite structure. We interpret this enhancements to a transition from unconnected particles to a connected high aspect ratio network structure of the fillers, as a result of sintering between silver particles after effective particle agglomeration through diffusion limited aggregation (DLA) and subsequent PVP removal. The resulting self-constructed tree-like metallic network yields the highest κ, surpassing the state of the art in polymer nanocomposites and opening up a new venue for designing high κ composites.

Supporting Information

Raman Spectroscopy of particles with and without PVP coating, morphology of uncoated particles, curing time of samples presented in Figure 2, optical microscopy images studying the effect of processing time and temperature on nanocomposite agglomeration, measurement results of viscosity versus time for pure epoxy and 20 vol% silver-epoxy nanocomposite, theoretical determination of the agglomeration time, and DSC curve of pure bulk PVP are presented in supporting information.

AUTHOR INFORMATION

Corresponding Author: *E-mail: borcat@rpi.edu.

Acknowledgement

We gratefully appreciate support from an IBM gift and the National Science Foundation under grant CBET 0348613.

References:

(1) Njuguna, J.; Pielichowski, K. *Adv. Eng. Mater.* **2003**, *5*, 769-778.

(2) Siow, K. S. *J. Alloys Compd.* **2012**, *514*, 6-19.

(3) Potara, M.; Jakab, E.; Damert, A.; Popescu, O.; Canpean, V.; Astilean, S. *Nanotechnol.* **2011**, *22*, 135101.

(4) Prasher, R. *Proc. IEEE* **2006**, *94*, 1571-1586.

(5) Hwang, S.; Jeong, S. *J. Nanosci. Nanotechnol.* **2011**, *11*, 610-613.

(6) Huang, X.; Jiang, P; Xie, L. *Appl. Phys. Lett.* **2009**, *95*, 242901.

(7) Balachander, N.; Seshadri, I.; Mehta, R. J.; Schadler, L. S.; Borca-Tasciuc, T.; Keblinski, P.; Ramanath, G. *Appl. Phys. Lett.* **2013**, 102, 093117.

(8) Liu, L.; Peng, Q.; Li, Y. *Nano Res.* **2008**, 1, 403-411.

(9) Mueller, S.; Llewellin E.W.; Mader H. M. *Proc. R. Soc. London, Ser. A* **2010**, *466*, 1201-1228.

(10) Hu, A.; Guo, J. Y.; Alarifi, H.; Patane, G.; Zhou, Y.; Compagnini, G.; Xu, C. X. *Appl. Phys. Lett.* **2010**, *97*, 153117.

(11) Perelaer, B. J.; de Laat, A. W. M.; Hendriks, C. E.; Schubert, U. S. *J. Mater. Chem.* **2008**, *18*, 3209-3215.

(12) Seo, D. S.; Park, S. H.; Lee, J. K. *Curr. Appl Phys.* **2009**, *9*, S72-S74.

(13) Lei, T. G.; Calata, J. N.; Lu, G.-quan; Chen, X.; Luo, S. *IEEE Trans. Compon. Packag. Technol.* **2010**, *33*, 98-104.

(14) Pashayi, K.; Fard, H. R.; Lai, F.; Iruvanti, S.; Plawsky, J.; Borca-Tasciuca, T. *J. Appl. Phys.* **2012**, *111*, 104310.

(15) Heo K.; Miesch C.; Emrick, T.; Hayward R. C. *Nano Lett.* **2013**, *13*, DOI: 10.1021/nl402813q

(16) Hamdan, A.; Cho, J.; Johnson, R.; Jiao, J.; Bahr, D.; Richards, R.; Richards, C. *Nanotechnol.* **2010**, *21*, 015702.

(17) Moon, K.-S.; Dong, H.; Maric, R.; Pothukuchi, S.; Hunt, A.; Li, Y.; Wong, C. P. *J. Electron. Mater.* **2005**, *34*, 168-175.

(18) Weber, A. P.; Friedlander, S. K. *J. Aerosol Sci.* **1997**, *28*, 179-192.

(19) Witten Jr., T. A.; Sander, L. M. *Phys. Rev. Lett.* **1981**, *47*, 1400-1403.

(20) Qin, X.; Zhiying, M.; Fang, Y.; Zhang, D.; Ma, J.; Zhang, L.; Chen, Q.; Shao, X. *Langmuir* **2012**, 28, 5218-5226.

(21) Ding, C.; Tian, C.; Krupke, R.; Fang, J. *Cryst. Eng. Comm.* **2012**, 14, 875-879.

(22) Wei, G.; Nan, C.-W.; Deng, Y.; Lin, Y.-H. *Chem. Mater.* **2003**, 15, 4436-4441.

(23) Evans, W.; Prasher, R.; Fish, J., Meakin, P.; Phelan, P.; Keblinski P. *Int. J. Heat Mass Transfer* **2008**, *51*, 1431-1438.

(24) Shahil K. M. F., Balandin A. A. *Nano Lett.* **2012**, 12 (2), 861–867.

(25) Chen, Y., M., Ting J., M. *Carbon* **2002**, 40, 359–362.

(26) Tanaka, T.; Kozako, M.; Okamoto, K. *J. Int. Counc. Electr. Eng.* **2012**, 2, 90-98.